The influence of a Hamiltonian vibration versus a bath vibration on the 2D electronic spectra and Quantum Information of a homodimer.

Ben S. Humphries,[a] Dale Green,[a] and Garth A. Jones[a]

a) *School of Chemistry, University of East Anglia, Norwich Research Park, Norwich, NR4 7TJ, UK*

Email: *b.humphries@uea.ac.uk*

Garth.Jones@uea.ac.uk

Introduction

Hierarchical equations of motion approaches (HEOM) non-perturbatively couple open quantum systems (OQS) directly to an harmonic environment and allow for non-Markovian dynamics. Here, through application of two test systems - the Hamiltonian and bath vibration models (HVM/BVM) - we demonstrate that the coupled, hierarchical structure of the HEOM can give rise to complex vibronic structure in 2D electronic spectra (2DES) when applied to dimer systems. Additionally, quantum information transfer and phonon transfer between different layers of the auxiliary density operator (ADO) hierarchy are connected to equivalent terms from the HEOM derivation.

Open Quantum Systems

The Hamiltonian for an OQS is split into the system (solute), the environment - or bath (solvent). The system of interest - in its most general form - is a tensor product of the electronic and vibrational degrees of freedom.

$$H=H_S+H_B$$

$$H_{mon} = |g\rangle \sum_{j=0,1} \left(\frac{p_j^2}{2m_j} + \frac{m_j\omega_j^2 q_j^2}{2} \right) \langle g| + |e\rangle \left(\hbar\omega_{eg}^0 + \sum_{j=0,1} \frac{p_j^2}{2m_j} + \frac{m_j\omega_j^2}{2}(q_j - d_j)^2 \right) \langle e|$$

$$H_{dim} = H_{mon}^{(1)} \otimes I_{mon}^{(2)} + I_{mon}^{(1)} \otimes H_{mon}^{(2)} + J \sum_{\eta_1,\eta_2} (|e,\eta_1,g,\eta_2\rangle \langle g,\eta_1,e,\eta_2| + c.c.)$$

The bath is defined[1] as a linear combination of delta functions, the profile of which is a continuous spectral density function.

$$J(\omega) = \sum_\alpha \frac{g_\alpha^2}{2m_\alpha\omega_\alpha} \delta(\omega - \omega_\alpha)$$

HVM and BVM

The Hamiltonian vibration model (HVM) contains explicit vibrational levels, in the BVM this is subsumed into the spectral density. ‘g’ is the ground state, e^+ and e^- are the bright and dark exciton states with a coupling of J, and ‘f’ is the doubly excited state.

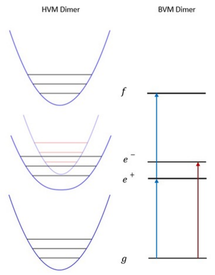

Fig 1: HVM/BVM dimer Energy level diagram.

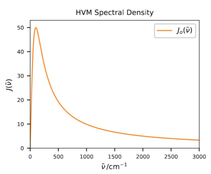

Fig 2: HVM spectral density

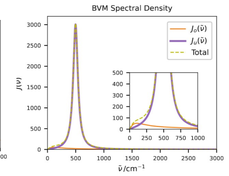

Fig 3: BVM spectral density and its components

Quantum Information Channels and Non-Markovianity

A quantum information channel is a map between two spaces of operators which corresponds to a ‘route’ of transmission for quantum - and classical - information. For two Hilbert spaces, L, ϕ is an information channel. An example in the Schrödinger picture is the time evolution of the density matrix.

ϕ: L(H_a) ⟶ L(H_b) | ρ ⟶ UρU*

Here, information is the complement of the observable entropy. Non-Markovian recurrence of information can be considered dependent on $\rho^{+/-}_{j,k,n}$. Quantum information channels exist in the bath allowing information flow via the orange and cyan couplings in the hierarchy.

The associated non-Markovianity,[2]

$$\mathcal{N} = \max_{\rho_s^{1,2}} \int_{\sigma>0} \sigma(t)\, \mathrm{d}t.$$

The information flux,[2] $\sigma = \frac{\mathrm{d}}{\mathrm{d}t}\left(\frac{1}{2}\mathbf{Tr}|\rho_1 - \rho_2|\right)$.

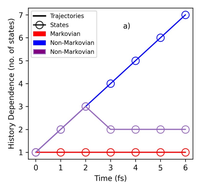

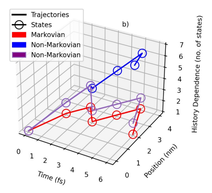

Fig 4: a) Depicting Markovianity. Markovian 1D lines due to zero gradient
b) explicit positional variation within the state trajectory.

Hamiltonian Vibration model, and Spectral Vibration Model

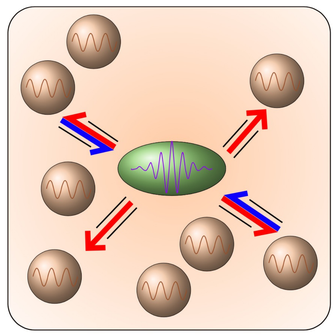

Fig 5: Diagram depicting a dimer interacting with a bath. Case 1, RHS: bath is purely overdamped. Case 2, LHS: underdamped bath due to the addition of the system vibration. Red and blue arrows depict Markovian and non-Markovian information flow respectively along the quantum information channels in black.

Fig 6: HVM and BVM flow diagram.[3] The intramolecular vibration of interest is either coupled to the Hamiltonian electronic states, or subsumed within an underdamped bath.

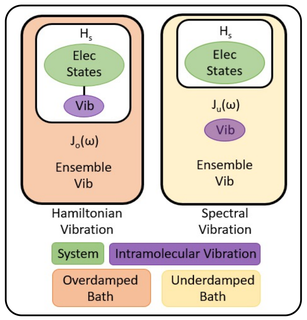

2DES Bath Vibration Model and Hamiltonian Vibration Model

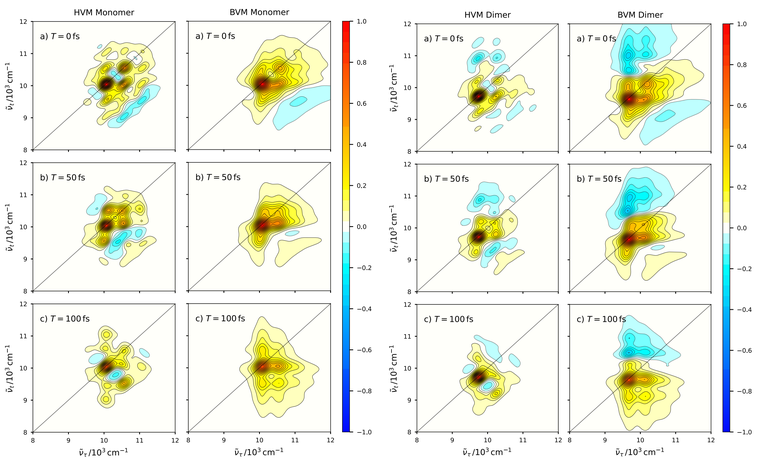

Fig 7 (and 8):[3] Absorptive 2D spectra for the HVM(BVM) monomer at T = 0, 50, and 100 fs, normalized to the maximum at T = 0 fs.

Fig 9 (and 10):[3] Absorptive 2D spectra for the HVM(BVM) dimer at T = 0, 50, and 100 fs, normalized to the maximum at T = 0 fs. J = -400 cm^{-1}

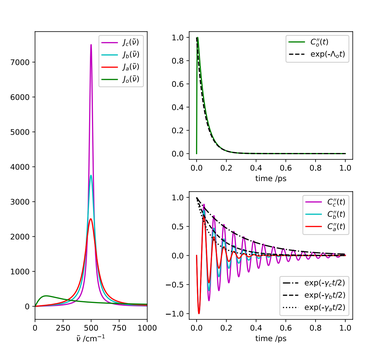

Fig 11 (and 12):[3] Spectral densities and correlation functions and associated BVM monomer absorptive 2D spectra for given γ

The HVM dimer spectra show full vibronic quenching whereas the BVM dimer exhibits a full -400 cm^{-1} redshift

In the limit γ → 0 additional 2DES peak broadening due to n ≥ 1 baths reduces.

Hierarchical Equations of Motion

Using an underdamped spectral density, $J_u(\omega)$, it is possible to derive[4] an hierarchy of equations of motion which can account for non-Markovian memory effects in the OQS. The hierarchy of ADOs has significant power over the dynamics: red terms represent Markovian dynamics of the free propagation of the system, blue terms describe non-Markovian free propagation of the bath, the orange highlighted terms behave similar to ‘lowering’ from higher ADOs and the cyan behave like ‘raising’ from lower ADOs.

$$\dot{\rho}_{\mathbf{j}}(t) = -\left(\mathcal{L} + \sum_{k=0}^{M} j_k\nu_k - \sum_{k=M}^{\infty} \hat{V}_S^\times \hat{\Psi}_k\right)\rho_{\mathbf{j}}(t) + \sum_{k=0}^{M} \hat{V}_S^\times \rho_{j_k^+}(t) +$$

$$j_0\hat{\Theta}^-\rho_{j_0^-}(t) + j_1\hat{\Theta}^+\rho_{j_1^-}(t) + \sum_{k=2}^{M} j_k\nu_k\hat{\Psi}_k\rho_{j_k^-}(t),$$

Termination[5] upon reaching convergence parameter, ξ, at assumed Markovian limit

$$\hat{\Psi}_k = \frac{4\eta}{\hbar\beta} \frac{\gamma\omega_0^2}{(\omega_0^2 + \nu_k^2)^2 - \gamma^2\nu_k^2} \hat{V}_S^\times,$$

$$\hat{\Theta}^\pm = \frac{\eta\omega_0^2}{2\zeta}\left\{\mp\hat{V}_S^\circ \pm \coth\left(\frac{\hbar\beta}{2}\left(\mp\zeta + i\frac{\gamma}{2}\right)\right)\hat{V}_S^\times\right\}$$

$$\frac{2(M+1)\pi}{\hbar\beta} > \xi, \quad \sum_{k=0}^{M} j_k|\mathbf{Re}(\nu_k)| > \xi.$$

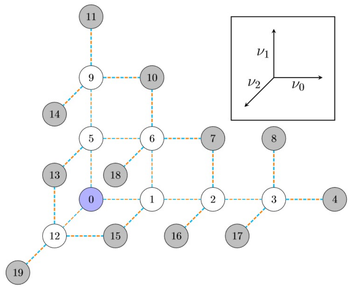

Fig 13: An hierarchy diagram for the HEOM showing connections between ADOs. Grey nodes are termination ADOs, cyan lines move towards the density matrix, orange move away

$$C(t) = \sum_{k=0}^{M} c_k e^{-\nu_k t}.$$

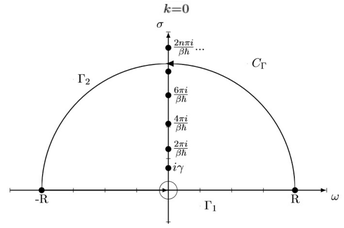

Fig 14: A complex contour in frequency space used to solve the correlation function. Residues of the poles correspond to Matsubara frequencies.

ADO structure diagram and Information metrics

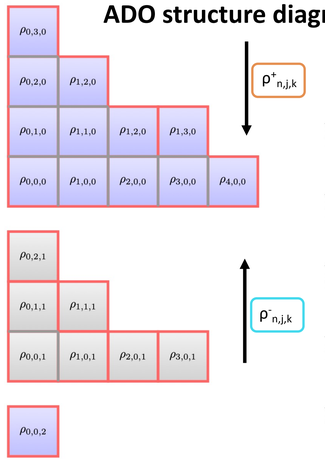

ρ0,0,0 non-Markovian information flux

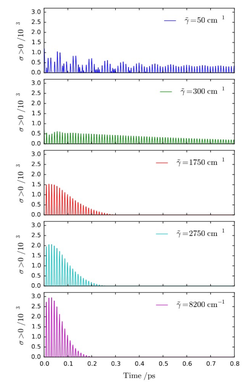

Fig 16:[6] Measured BLP associated with the information flux of the true density matrix for five bath speeds. $\Delta\tau_c$ is quoted for overdamped environments along with the FWHM of corresponding 2DES peaks.

Fig 15: ADO structure diagram for information flow. Red boundaries indicate information and phonons cannot transfer, grey and blue allow transfer up and down but the latter restricts transfer to the sealed hierarchy volume.

$\tilde{\gamma}$ /cm^{-1}	$\Delta \cdot \tau_c$	$\mathcal{N}$	FWHM (±1) /cm^{-1}
50	-	0.147	4
300	-	0.104	19
1750	0.64	0.052	110
2750	1.00	0.063	144
8200	3.00	0.074	196

Summary

The choice of the system–bath boundary placement clearly alters the vibronic coupling effects, as is evidenced by the lack of vibronic quenching relative to the Hamiltonian eigenvalues for the BVM. It is clear from these results that HVM vs BVM is a choice between energetic informational precision (peak position) and greater dynamic broadening, respectively. This represents a shift in the focus from an accurate system Hamiltonian to a model that efficiently includes a more complete system–bath interaction. This research was carried out on the ADA Cluster supported by the Research and Specialist Computing Support service at UEA.

References

1. M. Tanaka and Y. Tanimura, J. Phys. Soc. Jpn. 78, 073802 (2009)
2. E.-M. Laine, J. Piilo, and H.-P. Breuer, Phys. Rev. A 81, 062115 (2010)
3. B. S. Humphries, D. Green, G. A. Jones, Journal of Chemical Physics 156, 084103 (2022)
4. Y. Tanimura and R. Kubo, Journal of the Physical Society of Japan 58, 101 (1989).
5. A. G. Dijkstra and V. I. Prokhorenko, Journal of Chemical Physics147, 1 (2017)
6. D. Green, B. S. Humphries, A. G. Dijkstra, and G. A. Jones, Journal of Chemical Physics 151, 1 (2019).

Future Research

- Further derivations of HEOM and new HEOM variants
- Application of information metrics – BLP measure, coherence measures, and G2 tensor – to the system ADOs
- Comparisons with ASD-HEOM and generalised HEOM

Which may require additional computational power to realise